International Journal of Advanced and Applied Sciences, 6(4) 2019, Pages: 75-80

Contents lists available at Science-Gate

International Journal of Advanced and Applied Sciences

Journal homepage: http://www.science-gate.com/IJAAS.html

Theoretical and experimental analysis of the main girder double girder bridge cranes

Muamer Delić *, Nedim Pervan, Mirsad Čolić, Elmedin Mešić

Mechanical Engineering Faculty, University of Sarajevo, Sarajevo, Bosnia and Herzegovina

ARTICLE INFO

Article history:
Received 20 November 2018
Received in revised form
11 February 2019
Accepted 11 February 2019

Keywords:
Bridge crane
Main girder of crane
Theoretical analysis of girder
Experimental analysis

ABSTRACT

When designing cranes, it is necessary to analyze the value of the contraction of the construction, as well as the values of the maximum stresses occurring in the crane construction. Precisely, in this paper, the theoretical and experimental analysis of the contraction and stress condition of the main crane girder in accordance with the standard of crane-general design has been done. The analysis of mechanical appearance in the main girder of the crane is carried out on the basis of the analytic solution of equilibrium equations. The results obtained by the theoretical analysis of the main crane girder were verified by experimental tests on the model of a double girder bridge crane with a capacity of 250 kg. At the end of the work an analysis of the obtained results was performed, on the basis of which specified conclusions were made.

1. Introduction

Bridge cranes are used for handling in large workshops or storage. Usually working under the roof, and if necessary in the open. They move by two parallel rails placed along the length of the hall or storage on pillars or consoles. The main parts are, bridge and the driving winch, which moves along of the bridge. The movement of cranes (of the bridge) on the rails and the driving winch (carts) across the bridge to transport from one place to another within the working range of the crane (Delić et al., 2017). When designing cranes, it is necessary to analyze the value of the contraction of the construction, as well as the values of the maximum stresses occurring in the supporting crane construction. There are many published studies on structural and component stresses, safety under static loading and dynamic behaviour of cranes (Alkin et al., 2005; Patel and Patel, 2013; Oguamanam et al., 2001; Gaska and Pypno, 2011; Chmurawa and Gąska, 2005; Wu, 2006; Sowa et al., 2017; Gašić et al., 2011; 2012). In this paper, the theoretical analysis of mechanical appearance in the main carrier of the crane is carried out in accordance with the standard CEN (2016a, 2016b, 2016c). Verification of the obtained results was carried out by experimental testing on the model of the bridge crane developed in the Laboratory for Transporters at the Faculty of Mechanical Engineering in Sarajevo (Fig. 1).

Fig. 1: Model of bridge crane

On the model, it is possible to carry out various experimental tests to determine stress of the main girder, stress on the trolley winch, on wheels, up to the dynamics of lifting or moving.

The methods of experimental analysis enable the set of data important for structural analysis. This particularly applies to: optimization of shape and dimensions, effect of local stress concentration, the influence of change in mechanical properties of materials due to temperature changes, rating of bearing capacity and structural stability, and detecting areas of plasticity. Experimental methods are especially pronounced in cases where difficulties arise due to the complexity of the problem in its theoretical and numerical solution. Most commonly,

* Corresponding Author.
Email Address: delic@mef.unsa.ba (M. Delić)
https://doi.org/10.21833/ijaas.2019.04.009
Corresponding author's ORCID profile:
https://orcid.org/0000-0002-3943-4995

these are the places of singularity and high concentration of stresses (by a cut, a change of shape, the action of concentrated forces) which are often the cause of the damage, especially if the load is dynamic, exceeds the permissible value by entering the elastoplastic area or there is a strong temperature change.

2. Theoretical analysis

Analytical calculation and adoption of the IPE 80 profile as a profile for the main girder and solving simple static problems, (Fig. 2), (Repčić and Čolić, 2008; Hellmut, 1996).

$$\frac{M_{smax}}{W_y} \leq \sigma_d \tag{1}$$

where; σ_d: Permissible bending stress; W_y: Resistant moment of inertia (long-axis) I profile; M_{smax}: Maximum bending moment.

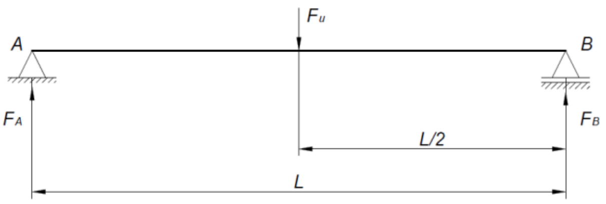

Fig. 2: The problem presented as a static designed

We have come to bearing capacity profile of 6, 4 kN. Checking carrier IPE 80 to lateral torsional buckling over expression:

$$\sigma_{max} \leq \frac{\sigma_D}{v} = \alpha_p \cdot \chi_D \cdot \frac{\sigma_v}{v} \tag{2}$$

where; σ_{max}: Maximum bending stress; σ_D: Marinal stress of torsional buckling; $v = 1.5$ Degree of safety; α_p: Coefficient of cross-sectional shapes; χ_D: Nondimensional coefficient of lateral torsional buckling. In this calculation we have less capacity profiles IPE 80 which amounts to 4.8 kN. Because the purpose crane was taken to its load capacity of 2452.5 N (250 kg).

2.1. Dimensioning of carts winch

As noted in the previous section it is established that the load capacity cranes are to be 250 kg, on the basis of which we dimension the carts winch. Their design is simple, consisting of four carriers, two of which (carriers 1 and 2) are used to enable the movement of carts (installation of wheels), and the other two (carriers 3 and 4) to carry only winch. Fig. 3 shows the basic design of carts winches.

Based on Fig. 3 we started to a structural analysis of the problem, which is determined by a cross-section of each carrier, and adopted the optimum corresponding to all carriers. The first step was to calculate carrier 3 because it is directly connected to the winch and load winch lifted, setting simple static problem, shown in Fig. 4. We can reach the dimensions of the cross section (because construction carts will work with square pipes and material S235JR). The dimension h corresponds to the range of the bridge, which was adopted in part 2.

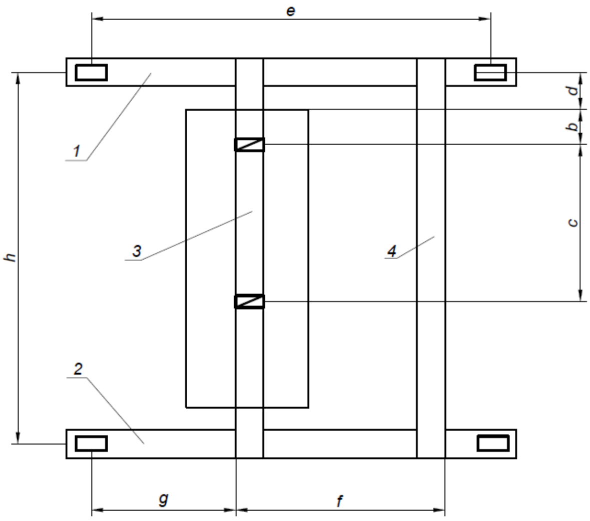

Fig. 3: Carts winch

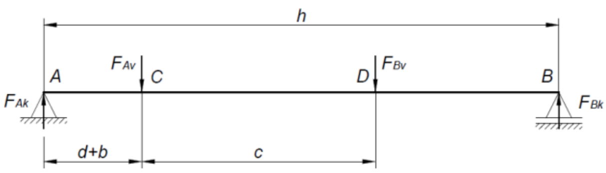

Fig. 4: Carrier winch as beams with two supports and two forces

By setting static equation for the problem in Fig. 4 we have,

$$\sum M_B = 0 \tag{3}$$
$$F_{Ak} \cdot h - F_{Av} \cdot [h - (d + b)] - F_{Bv} \cdot [h - (d + b + c)] = 0$$

The second equation would be that the sum of the vertical force equals zero,

$$F_{Ak} - F_{Av} - F_{Bv} + F_{Bk} = 0 \tag{4}$$

From the two previous equations we determined the reaction in supports A and B. On the basis of a reaction and the expression for the allowed stress,

$$\sigma_s = \frac{M_{smax}}{W_y} \leq \sigma_d \tag{5}$$

where; σ_s Bending stress; M_{smax} Maximum bending moment; W_y Resistant moment of inertia; σ_d Permissible stress for the selected material (16 kN/cm^2).

From equation (5) we calculated value resistant moment of inertia, and based on these values adopted a square tube dimensions 40x40x2. For other carriers (1, 2 and 4) we have made the same calculation. Also for all the carriers where adopted the same cross-sectional dimension pipes.

After dimensioning trolley winches, by Andrea method determining the pressures on the same wheels are designed for a specific trolley winch shown in Fig. 5.

The resultant force R corresponding to the maximum load capacity of the winch and it is 2452.5 N. The pressure at the trolley winch can be calculated at any point by the expression,

$$T'_i = \frac{R}{4bc} P_i, \qquad i = 1, \dots, 4 \tag{6}$$

where,

$P_1 = (b + x)(c + y)$ $P_3 = (b - x)(c - y)$
$P_2 = (b + x)(c - y)$ $P_4 = (b - x)(c + y)$

If we introduce the known values we will get pressures on wheels 1, 2, 3 and 4, and they amount to,

$T_1 = 1080.2$ N $T_4 = 319.5$ N
$T_2 = 821.6$ N $T_3 = 243.4$ N

Using force to wheels 1 and 2 we will check the main carrier (check stress and deflection).

As the wheels 1 and 2 are in direct contact with one main carrier crane which in this case is more burdened than the other carrier, forces from the wheels are transferred directly to the carrier, as shown in Fig. 6.

By setting up a simple static of the equilibrium conditions we will come to the value of reactions in supports for the main carrier. Then, over expression (5) we will determine the value of bending stress carrier in section I, and it is,

$$\sigma_{sI} = 39.58 \text{ MPa} < 160\ MPa$$

Here we also check the deflection over expression,

$$f = \frac{F}{3} \cdot \frac{L^3}{E \cdot I_y} \cdot \left(\frac{a}{L}\right)^2 \cdot \left(\frac{b}{L}\right)^2 \le \frac{1}{750} \cdot L \tag{7}$$

where; F: Force from wheel T_1 and T_2; L: Length of carrier E = 210 GPa: Modulus of elasticity for steel; I_y = 80 cm^4 Moment of inertia of the axis y.

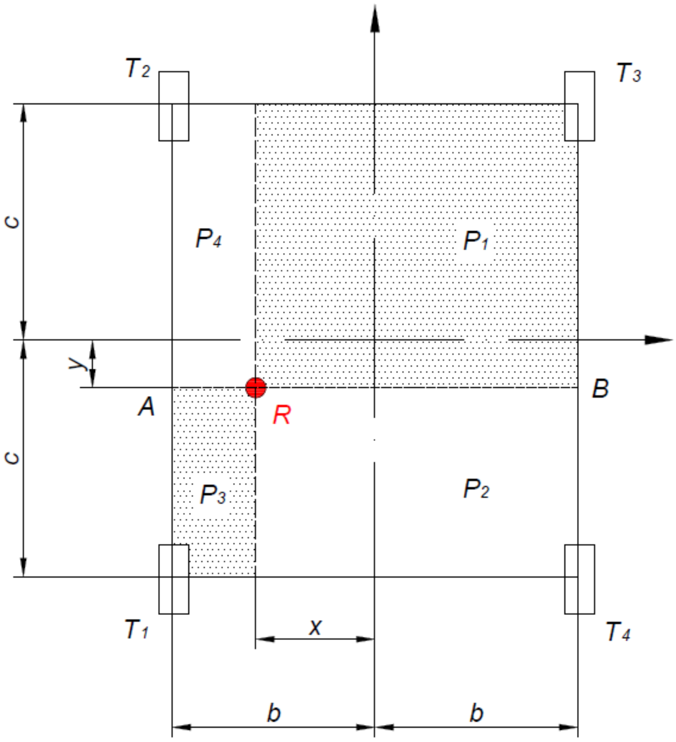

Fig. 5: Determination of pressure in the wheels trolley winch

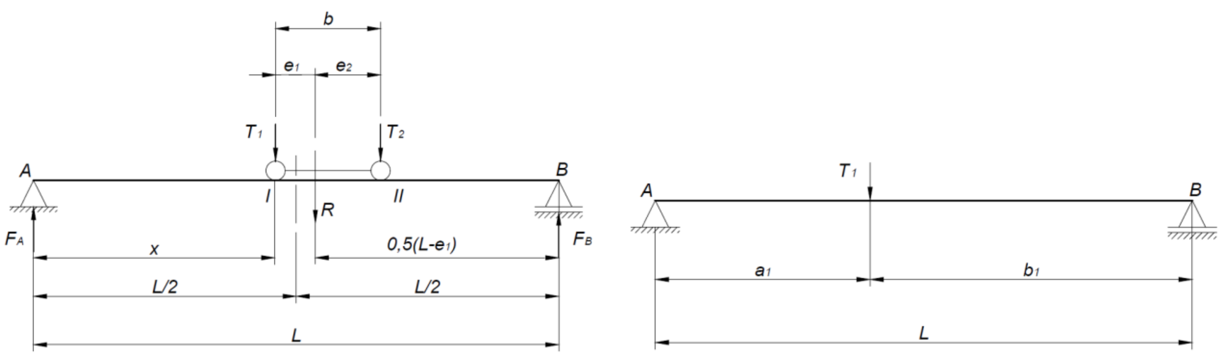

a **b**

Fig. 6: The carrier burdened with forces of the wheels 1 and 2 (a); Deflection of carrier with force T_1 (b)

We have two cases, first with load T_1 second with T_2. First case is shown in Fig. 6b.

$$f_1 = \frac{T_1}{3} \cdot \frac{L^3}{E \cdot I_y} \cdot \left(\frac{a_1}{L}\right)^2 \cdot \left(\frac{b_1}{L}\right)^2 \leq \frac{1}{750} \cdot L \quad (7)$$

where; L = 2 m: Length of carrier

$a_1 = 0.5\ (L - e_1) = 0.913$m
$b_1 = l - a_1 = 2 - 0.913 = 1.087$m

In the same way we get a deflection of force T_2 and deflection amounted,

$f_1 = 1.052\ mm$
$f_2 = 0.67\ mm$
$f = f_1 + f_2 = 1.72\ mm$
$f = 1.72 < \frac{1}{750} \cdot 2000 = 2.66\ mm$

3. Experimental analysis

3.1. Production of a model bridge crane

The model of the crane was made according to the technical documentation obtained on the basis of the analytical calculation. The model has all the necessary elements for lifting the load and move it from one place to another (Alkin et al., 2005). The main girder of crane are made of IPE 80 profile, 8x8 mm is a welded rod, which is used to guide the winch carriage. Carts winch made of pipe 40x40 mm.

The winch is mounted on the cart and has a load capacity of 250kg, these hoist elements are fully functional. Experimental test setting of the model bridge crane is shown in (Fig. 7). The crane is supported on two ends, one side is movable, the other immobilized, loaded with two forces corresponding to the force on the wheels 1 and 2.

Since it was emphasized that the model is as close as possible to the actual crane, it was necessary to provide the movement of the winch carts. Models of wheelchairs winch were developed as well as their technical documentation, (Fig. 8).

Fig. 7: Experimental test setting of the model bridge crane

Fig. 8: Model wheel of carts winch

The accent was on the possibility of installing an electric motor to drive the winch carts, which was done, movement of the winch carriages by the bridge is facilitated by an electric motor that drives two wheels of winch and thus allows the transfer of load from one place to another. Since the wheel was loaded by the force of the pressure from the load itself, it was necessary to calculate its diameter, it is calculated from the relation (8).

$$D_T \geq \frac{F}{p_{dr} \cdot k_2 \cdot k_3 \cdot (b_0 - 2 \cdot r)} \quad [\text{mm}] \quad (8)$$

where; $p_{dr} = p_{dur}$; k_{1r}: Permissible surface pressure point for a flat head shape of the rail; p_{dur} = 7.5 [Mpa]: Allowed conditional pressure; b_0 = 8 [mm] Width of the head of the rail; r = 0.5 [mm] Radius of the curve of the rail; k_{1r}, k_2, k_3: Coefficients

Based on the force F value, as defined in section 2, we obtain the diameter of the wheel $D_T = 45$ mm.

Also, it is necessary to dimension the shaft of the wheel that is loaded on load bending. This case can be seen as a beam with two supports as shown in Fig. 9. By solving well-known equations from the equilibrium conditions, we arrive at the reactions in the supports, and on the basis of the larger gain reaction and the shaft diameter using the relation (9). The adopted diameter of the shaft is $d = 8\ mm$.

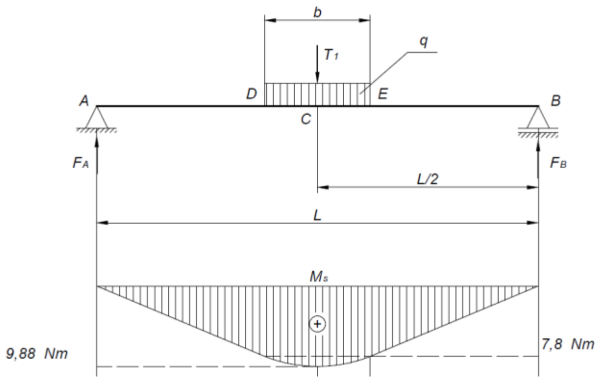

Fig. 9: Shaft whell load

$$\sigma_s = \frac{M_{smax}}{W_y} \leq \sigma_{doz} \quad (9)$$

3.2. Stress analysis of main girder with strain gauges

The most commonly used method in experimental stress analysis is the method of electro-resistance measurements (strain gauge). Before placing the measuring tape on the work piece, it is necessary to have the surfaces on which the measuring strips will be completely cleaned from corrosion, grease and other impurities that would menace their proper leakage to the surface. Our profile at the place of the tape is brushed and cleaned by medical alcohol of all impurities.

The electro-resistant strain gauges for the steel 6/120LY11 marker manufacturer HBM (Fig. 10) have been used with the following characteristics (Pervan et al., 2017):

- Resistance: 120 Ω ± 0,35%,

- Active length of the strain gauge: 6 mm,
- Tape factor (k-factor): 2.03 ± 1%,

The active strain gauge must be placed exactly below the loaded wheel, or at the point where we have reached the stress value by analytical calculation. The passive (compensating) strain gauge is placed where the deformations and the stresses are equal to zero and serves only to compensate for the influence of the temperature on the accuracy of the measurements.

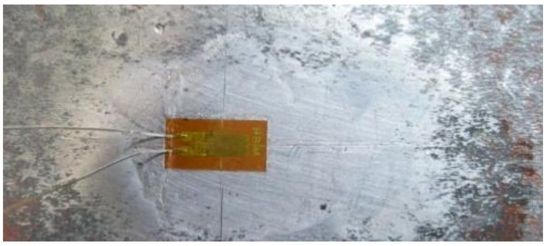

Fig. 10: Active strain gauge

Fig. 10 shows the glued active strain gauge. Since in our case we have two strain gauge (one active and one compensatory), it is clear that when we connect, we will use the Wheatstone half-bridge configuration whose scheme is shown in Fig. 11.

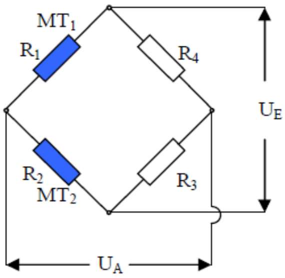

Fig. 11: Wheatstone half-bridge configuration

After this, we connect the strain gauge to the measurement-amplification system and through the computer and the software we come up with deformation data.

The deformation given by Wheatstone's half-bridge with one active and one compensatory measuring tape is given by the relation (Mešić et al., 2014; 2016; 2015):

$$\varepsilon = \frac{4}{k_m} \cdot \frac{U_A}{U_E} \tag{10}$$

where: k_m: Strain gauge factor; U_A: Voltage at the output of the Wheatstone Bridge; U_E: The supply voltage of the Viston Bridge.

Fig. 12 shows a diagram showing the change in the deformation of the strain gauge in time, after some time and the deformation stabilization, we can read the exact value.

In the time frame between the 170s and 220s there is a dynamic load, but here we consider the result when the loaded system is brought into a calm state. This opens the possibility of further research related to the dynamics of the bridge crane. The deformation value we read in the software is:

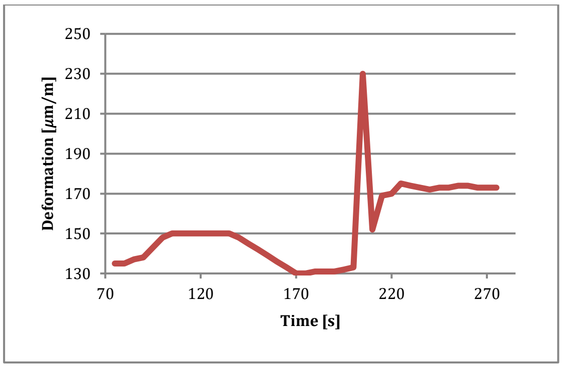

Fig. 12: Deformation diagram of strain gauge

$\varepsilon = 173.72 \quad [\mu m/m]$

Including this value into the expression (11), we obtain the bending stress value on the main girder of the model crane:

$$\sigma_s = \varepsilon \cdot E \quad [\text{MPa}] \tag{11}$$

where: ε: Deformation read in the software; E = 210 Gpa: Modulus of elasticity for steel.

4. Results

In the analytical calculation, the results are related to the ideal condition of the construction, while experimental tests give results that are influenced by many factors, such as load type, setting limits on girder support, the conditions under which the test was carried out, temperature, dampness and many other factors.

If we compare the obtained analytical and experimental results (Table 1), we can notice that the deviation is 8.4%, which is satisfactory, taking into account the complexity of the construction itself.

Table 1: Results of analysis

	Stress (MPa)
Analytical results	39.58
Experimental results	36.5

5. Conclusion

In this paper we make a comparison of the theoretical analysis and experimental tests of the main girder of the bridge crane model. The theoretical analysis of mechanical phenomena in the main girder of the crane is in accordance with the standard CEN (2016a, 2016b, 2016c). The verification of the obtained results by the theoretical analysis was carried out by experimental testing on a bridge crane model with a load capacity of 250 kg. When designing a model crane, it is necessary to keep in mind the space in which the crane will work, taking care of these limitations, the length of the crane bridge and the bridge clearance are dimensioned. All checks on the main and side girder are met. The same stress we see that there is a deviation in the result of 8.4%, which, given the complexity of the construction itself, is satisfactory.

Compliance with ethical standards

Conflict of interest

The authors declare that they have no conflict of interest.

References

Alkin C, Imrak CE, and Kocabas H (2005). Solid modeling and finite element analysis of an overhead crane bridge. Acta Polytechnica, 45(3): 61-67.

CEN (2016a). EN 13001–1: Cranes- general design- Part 1: General principles and requirements. European Committee for Standardization, Brussels, Belgium.

CEN (2016b). EN 13001–2: Cranes- general design- Part 2: Load actions. European Committee for Standardization, Brussels, Belgium.

CEN (2016c). EN 13001–3.1: Cranes- general design- Part 3.1: Limit states and proof of competence of steel structure. European Committee for Standardization, Brussels, Belgium.

Chmurawa M and Gąska D (2005). Modeling of bridge cranes for dimensioning needs of their load-carrying structures. The International Journal of Ingenium, Cracow–Glasgow–Radom, 4: 409-414.

Delić M, Colic M, Mešic E, and Pervan N (2017). Analytical calculation and FEM analysis main girder double girder bridge crane. TEM Journal, 6(1): 48-52.

Gaska D and Pypno C (2011). Strength and elastic stability of cranes in aspect of new and old design standards. Mechanics, 17(3): 226-231. https://doi.org/10.5755/j01.mech.17.3.495

Gašić V, Zrnić N, and Petković Z (2012). Dynamic responses of a gantry crane structure due to an acceleration moving mass. In the International Conference on Material Handling, Construction and Logistics, MHCL, 12(XX): 113-118.

Gašić V, Zrnić N, Obradović A, and Bošnjak S (2011). Consideration of moving oscillator problem in dynamic responses of bridge cranes. FME Transactions, 39(1): 17-24.

Hellmut E (1996). Die Hebezeuge-band II- Winden und krane, Friedr. Vieweg i sohn, Braunschweig, Germany.

Mešić A, Čolić M, Mešić E, and Pervan N (2016). Stress analysis of chain links in different operating conditions. International Journal of Engineering Science Invention, 5(12): 43-49.

Mešić E, Avdić VA, and Pervan N (2015). Numerical and experimental stress analysis of an external. Folia Medica Facultatis Medicinae Universitatis Saraeviensis, 50(1): 52-58.

Mešić E, Vahid, A, Nedim P, and Nedžad R (2014). Finite element analysis and experimental testing of stiffness of the Sarafix external fixator. In the 25th DAAAM International Symposium on Intelligent Manufacturing and Automation, Procedia Engineering, 100: 1598-1607.

Oguamanam DCD, Hansen JS, and Heppler GR (2001). Dynamics of a three-dimensional overhead crane system. Journal of Sound and Vibration, 242(3): 411-426. https://doi.org/10.1006/jsvi.2000.3375

Patel PR and Patel VK (2013). A review on structural analysis of overhead crane girder using FEA technique. Evaluation, 2(4): 41-44.

Pervan N, Mešić E, and Čolić M (2017). Stress analysis of external fixator based on stainless steel and composite material. International Journal of Mechanical Engineering and Technology, 8(1): 189-199.

Repčić N and Čolić M (2008). Transportna sredstva. Mašinski Fakultet, Belgrade, Serbia.

Sowa L, Saternus Z, and Kubiak M (2017). Numerical modelling of mechanical phenomena in the gantry crane beam. Procedia Engineering, 177: 225-232. https://doi.org/10.1016/j.proeng.2017.02.193

Wu JJ (2006). Finite element analysis and vibration testing of a three-dimensional crane structure. Measurement, 39(8): 740-749. https://doi.org/10.1016/j.measurement.2006.03.002